Spectrum Sensing for Cognitive Radios in Time-Variant Flat-Fading Channels: A Joint Estimation Approach

Bin Li, Chenglin Zhao, Mengwei Sun, Zheng Zhou, *Member, IEEE*, and Arumugam Nallanathan, *Senior Member, IEEE*

***Abstract*—Most of the existing spectrum sensing schemes utilize only the statistical property of fading channels, which unfortunately fails to cope with the time-varying fading channel that has disastrous effects on sensing performance. As a consequence, such sensing schemes may not be applicable to distributed cognitive radio networks. In this paper, we develop a promising spectrum sensing algorithm for time-variant flat-fading (TVFF) channels. We first formulate a dynamic state-space model (DSM) to characterize the evolution behaviors of two hidden states, i.e., the primary user (PU) state and the fading gain, by utilizing a two-state Markov process and another finite-state Markov chain, respectively. The summed energy, which serves as the observation of DSM, is employed for the ease of implementation. Relying on a Bayesian statistical inference framework, the sequential importance sampling based particle filtering is then exploited to numerically and recursively estimate the involved posterior probability, and thus, the PU state and the fading gain are jointly estimated in time. The estimations of two states are soft-outputs, which are successively refined with a designed iterative approach. Simulation results demonstrate that the new scheme can significantly improve the sensing performance in TVFF channels, which, in turn, provides particular promise to realistic applications.**

***Index Terms*—Spectrum sensing, time-variant flat fading, dynamic state-space model, Beyesian statistical inference, joint estimation.**

I. Introduction

COGNITIVE RADIO (CR) enables dynamic spectrum access (DSA) and opportunistic transmission of the secondary user (SU) in authorized primary frequency bands [1], which is of great promise to promote the efficiency of frequency utilization and hence alleviate the scarcity of spectrum resources [2]–[4]. Based on a real-time awareness of operation surroundings and the bandwidth availability, CR can intelligently adapt its functionalities to best accommodate the current wireless environment and simultaneously best serve its users [2]. One of the most fundamental issues to be considered in CRs is spectrum sensing, which aims to identify the unknown working states (i.e., active or sleep) of primary user (PU) and, therefore, makes the SUs ready for the opportunistic use of vacant primary bands [5], [6].

Traditional spectrum sensing techniques include energy detection (ED) [7], matched filter (MF) detection [8] and cyclostationary feature detection [10], [11], which in practice may have different advantages and requirements [5], [6]. ED excludes any *a priori* information of PU signals and, therefore, is robust and simple, which yet has an uncompetitive sensing performance [9], [12]. In coherent MF detection, pilot signals are employed to achieve the optimum detection performance [8], which, however, may impractically require the perfect timing and the complete waveform (or sequence) information of PUs. By concentrating on the spectrum correlation function (SCF) of primary signals, cyclostationary detection may identify spectrum holes even in extremely low signal to noise ratio (SNR). However, the exhaustive search for unknown cyclic frequency makes it computationally intensive [5].

Recently, wavelet analysis [13] and compressive sensing are introduced to perform multi-band sensing [14]. By properly exploiting the statistical information of primary signals, a covariance-matrix based sensing algorithm is developed in [15], which has been proven to be efficient and robust in realistic applications [16]. It is noted that, by exploiting statistical correlations of PU signals (e.g., the time or spatial correlations), this covariance-based method may significantly improve the sensing performance. As suggested, the probabilistic property of PU's states may be utilized either to optimize the sensing strategy and thereby maximize the throughput of CR networks [17], or to design the sensing algorithm and further enhance the sensing performance [18].

From a general system point of view, the spectrum sensing may involve three stochastic processes, i.e., the contaminated PU signal x (or noise z), the random channel state α and the observation (or decision) variable y (e.g., the summed energy). The observation variable is closely coupled with the other two random components, relying on which the spectrum sensing is realized. Practically, the channel state is independent of the PU state, as far as the purpose of spectrum sensing is concerned.

Manuscript received August 23, 2013; revised December 26, 2013 and March 20, 2014; accepted May 7, 2014. Date of publication May 20, 2014; date of current version August 20, 2014. This work was supported by the National Science and Technology Major Project under Grant 2013ZX03001015-003, by NSFC under Grants 61379016 and 61271180, by the Doctoral Fund of Ministry of Education of China under Grant 20130005110016, by the Fundamental Research Funds for the Central Universities under Grant 2014RC0101, and by the Ministry of Knowledge Economy (MIKE), Korea, under the Information Technology Research Center (ITRC) support program supervised by the NIPA (NIPA-2011-C1090-1111-0007). The associate editor coordinating the review of this paper and approving it for publication was H. Li.

B. Li, C. Zhao, M. Sun, and Z. Zhou are with the School of Information and Communication Engineering, Beijing University of Posts and Telecommunications, Beijing, 100876 China (e-mail: stonebupt@gmail.com).

A. Nallanathan is with the Department of Informatics, King's College London, London WC2R2LS, U.K. (e-mail: nallanathan@ieee.org).

Color versions of one or more of the figures in this paper are available online at http://ieeexplore.ieee.org.

Digital Object Identifier 10.1109/TCOMM.2014.2325835

Hence, the unknown channel is only a latent variable for CR devices. It should be noteworthy that, nevertheless, such a latent variable will significantly increase the uncertainty of the observation variable y and, therefore, may have remarkable effects on the sensing performance. For the emerging CR applications with mobile devices (e.g., LTE-A and 802.11n), the channel may become time-variant [19], [20], making the spectrum sensing even tougher. In practice, the time-varying fading is not always an unfavorable factor. For example, the PU signal cannot be detected in extremely low SNRs regions. With proper configurations, however the statistical property introduced by time-varying fading effects may distinguish PU signals from the background Gaussian noise [21]. In such cases, the time-varying fading would become beneficial. In this investigation, notice that, the slow-varying fading is mainly considered, i.e., the dynamic gain remains invariant during a sensing slot, which may unfortunately degrade the performance.

In order to lower the adverse effects of fading channels, the more complicated cooperative diversity technique can be suggested as one feasible approach [22]–[24], which, however, may increase the complexity dramatically and in turns pose other challenges in practical deployments of distributed CR networks. Another common approach is to estimate the PU state relying on the marginal posterior probability $p(x|y) = \int_{\alpha} p(x, \alpha|y) d\alpha$, by averaging out the unknown channel [25]. In the case of more realistic time-varying flat fading (TVFF) channels [19], [20], [26], [27], these existing methods (i.e., ED) may become less attractive, even if the statistical property of fading channels may be exploited. This is because such sensing techniques are premised basically on a *static* system model [4]–[6]. So, in practice, the statistical probability distribution function (PDF) (e.g., Rayleigh distribution) can only characterize instantaneous random behaviors of the fading channel [25], which unfortunately fails to model or track the time-dependent evolutions of fading gains. More importantly, the *memory* exists widely in time-correlated channels [28], which may be exploited to enhance the receiving performance furthermore. Nevertheless, most existing sensing schemes can only focus on random but memoryless channels.

In this paper, we present a new spectrum sensing framework to address the tremendous difficulty posed by realistic TVFF channels. We employ a dynamically stochastic system model to characterize the spectrum sensing process, which is thereby formulated as a blind estimation problem. Relying on the Bayesian statistical inference and the Monte-Carlo simulated particle filtering (PF) [29], [30], the estimation of both the time-varying fading gain and PU state are jointly derived for distributed applications (i.e., non-cooperative case). To sum up, our main contributions in this work are two-fold.

A. Dynamic State-Space Model of Spectrum Sensing

Taking the dynamic evolutions of both PU states and the time-varying fading channels into accounts, a discrete dynamic state-space model (DSM) is established to effectively describe the realistic sensing process. In other words, two hidden states are considered in the new sensing model, i.e., the PU's working state and the real-time fading gain.

With regard to unknown PU state, we employ a two-state Markov chain to thoroughly characterize its dynamic behavior. An alternating renewal process is considered and the prior PDFs of PU states are further assumed to follow the exponential distribution. Thus, the time-dependent state transitional probability may be evaluated conveniently. Meantime, the continuously varying fading gain of TVFF channels is treated as another unobserved state. The finite state Markov chain (FSMC) is utilized to properly depict dynamic transitions of the correlated channel gains over times. Besides, in the formulated DSM the fading channel is also assumed to be data-independent, i.e., the PU state and the fading gains will evolve independently without affecting each other. The summed energy, which is used for implementation simplicity, is treated as the observation of two hidden states. The objective of spectrum sensing, therefore, is to estimate the PU state based on the noisy and nonlinear observations. It is expected that such a dynamic model could utilize the underlying channel memory more profoundly and hence may improve the sensing performance.

B. Joint Estimation Based Spectrum Sensing

Building on the new stochastic DSM and sequential Bayesian inference, a promising joint estimation algorithm is further designed to address the spectrum sensing in the presence of TVFF propagations. In sharp contrast to classical *threshold-based* techniques, in the proposed scheme the real-time fading gain will also be estimated recursively based on new observations (i.e., the summed energy), rather than only detecting the PU state by setting the threshold.

The new sensing algorithm mainly consists of three steps, i.e., coarse detection, fading gain update and PU state estimation. By designing an appealing iterative scheme (i.e., a *turbo-like* estimation method) in which the estimations of two hidden states are refined successively, the PU state and fading gain are estimated by maximizing the posterior probability. In order to realize recurrence estimations of the posterior density which cannot be analytically derived due to the underlying non-stationary DSM, the Monte-Carlo random sampling based particle filtering is further suggested. Premised on a promising sequential importance sampling (SIS) strategy, a group of discrete particles with evolving weights are employed to approximate the complicated density numerically. Thus, as the new observation comes, the non-analytic posterior probability can be recursively and numerically derived in time. With the assistance of the estimated fading gain, the sensing performance in realistic TVFF channels can be improved significantly by the proposed scheme, compared with other traditional methods which fail to exploit the underlying dynamics of time-varying fading channels.

The rest of this paper is structured as follows. A new DSM for spectrum sensing in realistic TVFF propagations is formulated in Section II. Subsequently, the sequential Bayesian detection and PF is briefly introduced in Section III. On this basis, by designing a turbo-like iterative estimation scheme, a promising sensing algorithm which jointly estimates the fading gain and PU state is proposed. In Section IV, the numerical experiments

and performance analysis of the new sensing algorithm are provided in realistic TVFF channels. Finally, we conclude the investigation in Section V.

II. System Model of Spectrum Sensing

By concentrating only on the time-invariant statistical PDFs, traditional sensing schemes may become seriously susceptible to realistic TVFF propagations. Accordingly, the sensing performance will be degraded significantly in such situations. In this section, we take the time-varying property of fading propagations into full consideration and formulate a more comprehensive dynamic model to characterize spectrum sensing in TVFF channels.

Before proceeding further, the sensing strategy adopted in this investigation should be specified firstly. Since SU cannot cause harmful interference to PUs when using the idle spectrum, they should identify the unused spectrum before establishing CR links. Meanwhile, as PUs may reclaim the authorized band any time, the SUs are also supposed to periodically sense in order to avoid interfering PU. Thus, the periodic sensing strategy is adopted in the analysis [3], [5]. That is, a fixed frame duration T_F is assumed, where the sensing duration is T_S and the remaining $T_F - T_S$ is used for data transmission.

A. PU Working State

Most investigations have revealed the working state of specific wireless networks may be practically modeled as an alternating renewal source. That is, the PDFs of both busy and idle states can be described by the exponential distribution [18], [31], [32], i.e.,

$$f_{S_1}(n) = \mu \times \exp(-\mu n) \tag{1a}$$

$$f_{S_0}(n) = \lambda \times \exp(-\lambda n) \tag{1b}$$

where μ and λ denote two transitional rates of state switches from busy to idle and from idle to busy, respectively. n is the discrete time index. With the help of *Komogorov* Equation, the probability of the idle state remaining unchanged during q successive slots, which is denoted by $p_{00}(q) \triangleq \Pr(s(n) = 0 | s(n-j) = 0, 1 \le j \le q)$, is given by:

$$p_{00}(q) = \frac{\mu}{\mu+\lambda} + \frac{\lambda}{\mu+\lambda} \exp\left[-q(\mu+\lambda)\right]. \tag{2}$$

Accordingly, the probability of the PU state handing over to busy in the qth detection period, after staying idle for $q-1$ periods, can be expressed as $1 - p_{00}(q)$. Similarly, the probability of the active state lasting for q slots, i.e., $p_{11}(q) \triangleq \Pr(s(n) = 1 | s(n-j) = 1, 1 \le j \le q)$, may be written to:

$$p_{11}(q) = \frac{\lambda}{\mu+\lambda} + \frac{\mu}{\mu+\lambda} \exp\left[-q(\mu+\lambda)\right]. \tag{3}$$

Thus, if we find the primary state staying in idle at the moment n_0 with a probability $\Pr(s_{n_0} = 1)$, then the probability that this PU state always stays in idle within q sensing slots is given by:

$$\Pr\left(s_{n_0+q} = 1 | s_{j\in[n_0+1, n_0+q-1]} = 1\right) = p_{11}(q) \times \Pr(s_{n_0} = 1). \tag{4}$$

More widely, for most wireless services, the evolution of the working states (i.e., active or sleep) over time is usually correlated and, therefore, may be abstracted by a finite state machine $\mathbb{S} = \{S_0, S_1\}$, i.e., a two-state Markov transition procedure [31]. To be specific, given that PU is in active state S_1 at the current sensing slot, then it will stay in S_1 with a probability of $p_{11}(1)$ and enter into sleep state S_0 with $p_{10}(1)$ in the next time slot. If it is currently in sleep state S_0, then it will stay in S_0 in the next slot with a probability of $p_{00}(1)$ and move to S_1 with $p_{01}(1)$. Obviously, we have:

$$p_{10}(1) = 1 - p_{11}(1),\ p_{01}(1) = 1 - p_{00}(1). \tag{5}$$

B. Time-Varying Fading Gain

A mobile Rayleigh fading channel is considered in the analysis, which has been widely adopted to characterize the time-varying fading effects [26], [33]. For a fixed time, the PDF of fading gain α is given by:

$$f(\alpha) = \frac{\alpha}{\sigma^2} \exp\left(-\frac{\alpha^2}{2\sigma^2}\right). \tag{6}$$

For most emerging applications involving mobile devices (e.g., LTE-A) or some specific environments with relative movements (e.g., indoor offices) [20], the fading gain of realistic CR links may become a time-varying random process [33]. In such cases, the dynamic behavior of fading gains α, which randomly evolves with times, can be usually characterized by two models, i.e., the autoregressive (AR) model [34] and the Clarke's model [35]. Rather, in this analysis we will consider another more versatile approach, known as the FSMC model, which is analytically tractable and may practically produce closed-form solutions. It is shown that the memory may remain widespread in slow-varying channels and, as has been verified, the Markovian transitional property of FSMC effectively reflects the dynamical nature of TVFF gains [33], [36], [37]. The FSMC model is also of practice use to receiver designs in the presence of TVFF channels, with which the underlying memory may be properly exploited to further promote the detection performance.

For the FSMC based fading channel, the representative discrete state at time index n', which is viewed as the output of a specific Markov chain [33], is denoted by $A_k \in \mathbb{A}, k \in \{0, 1, \ldots, K-1\}$. Correspondingly, the state transition can be specified by a transitional probability matrix (TPM) $\mathbf{\Pi}_{K\times K} = \{\Pi_{k_1 \to k_2}, k_1, k_2 \in 0, 1, \ldots, K-1\}$.

$$\mathbf{\Pi}_{K\times K} = \begin{bmatrix} \Pi_{0\to 0} & \Pi_{1\to 2} & \cdots & \Pi_{0\to(K-1)} \\ \Pi_{1\to 0} & \Pi_{1\to 1} & \cdots & \Pi_{1\to(K-1)} \\ \vdots & \vdots & \ddots & \vdots \\ \Pi_{(K-1)\to 0} & \Pi_{(K-1)\to 1} & \cdots & \Pi_{(K-1)\to(K-1)} \end{bmatrix}. \tag{7}$$

where each element $\Pi_{k_1\to k_2}$ accounts for the transitional probability from the state k_1 at time index $(n'-1)$ to the state k_2 at time index n':

$$\Pi_{k_1\to k_2} \triangleq \Pr\left(\alpha_{n'} = A_{k_2} | \alpha_{n'-1} = A_{k_1}\right). \tag{8}$$

With the wide-sense-stationary uncorrelated scattering (WSSUS), the time-correlation property is usually ergodic and stationary in practice [27]. Correspondingly, the FSMC model is also assumed to be stationary, which is shown to be reasonable in many practical scenarios with channel statistics changing slowly over time [33]. That is, each element $\Pi_{k_1\to k_2}$ is independent of time index n'. Furthermore, an indecomposable FSMC is considered in the analysis. I.e., if we denote the stationary probability vector $\boldsymbol{\pi} = [\pi_0, \pi_1, \ldots, \pi_{K-1}]^T$ with $\pi_k \triangleq \Pr(\alpha_n = A_k)$, then we have $\boldsymbol{\Pi}^T\boldsymbol{\pi} = \boldsymbol{\pi}$.

It should be emphasized that the amplitude of fading channel is of particular significance to spectrum sensing, as far as the widely adopted ED is concerned. So, we mainly concentrate on the modeling of time-varying fading gains by resorting to FSMC, while basically ignoring its phase characteristic. Thus, the nonnegative channel gain α may be partitioned into K non-overlapping regions, which is denoted by $\mathbb{V}$. If we further specify $\nu_0 = 0$ and $\nu_K = \infty$, we may have

$$\mathbb{V} = \left\{[\nu_0, \nu_1), [\nu_1, \nu_2), \ldots, [\nu_{K-1}, \nu_K)\right\}. \tag{9}$$

Correspondingly, the steady probability that the fading amplitude resides in the kth region can be derived from:

$$\pi_k = \int_{\nu_k}^{\nu_{k+1}} \frac{\alpha}{\sigma^2}\exp\left(-\frac{\alpha^2}{2\sigma^2}\right)d\alpha,\ 0 \le k \le K-1. \tag{10}$$

Under an equiprobable partition, i.e., $\pi_k = 1/K$, we may easily derive the partitioning bounds by $v_k = \sqrt{-2\sigma^2 ln(1-k/K)}$. Then, the transitional probability $\Pi_{k_1\to k_2}$ can be determined by

$$\begin{aligned}\Pi_{k_1\to k_2} =& \Pr\left\{\alpha_{n'} \in [\nu_{k_2}, \nu_{k_2+1}) | \alpha_{n'-1} \in [\nu_{k_1}, \nu_{k_1+1})\right\}\\ =& \frac{1}{\pi_{k_1}}\int_{\nu_{k_2}}^{\nu_{k_2+1}}\int_{\nu_{k_1}}^{\nu_{k_1+1}} f(\alpha_{n'-1}, \alpha_{n'})d\alpha_{n'-1}d\alpha_{n'}.\end{aligned} \tag{11}$$

where $f(\alpha_{n'-1}, \alpha_{n'})$ is the bivariate Rayleigh joint PDF described in [39], [40].

For simplicity, we further adopt the first-order FSMC model, which usually matches well with the popular statistical fading models (e.g., Clarke's model). Thus, the current fading channel state is only associated with the previous state while keeping statistically independent of all other past and future fading channel states, as is illustrated by Fig. 1. To be more specific, we have $\Pi_{k_1\to k_2} = 0$ for $|k_1 - k_2| > 1$. Therefore, the TPM $\boldsymbol{\Pi}_{K\times K}$ can be simplified into eq. (12), shown at the bottom of the page.

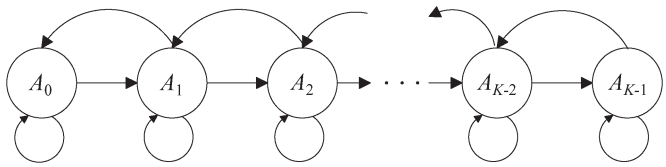

Fig. 1. The FSMC state transition model of the TVFF channel gains. Notice that the first-order FSMC is assumed, with the next transition state selected from the most adjacent states.

In practice, the level crossing rate (LCR) N_k may be utilized to evaluate the transitional probabilities numerically [28], [33], which refers to the number of times per second that the fading amplitude crosses ν_k in a downward direction [41]. For the Rayleigh fading, we may have

$$N_k \triangleq \int_0^\infty \dot{\alpha} f(\alpha, \dot{\alpha})d\dot{\alpha}|_{\alpha=v_k} = \sqrt{2\pi} f_D \frac{\nu_k}{\sigma}\exp\left(-\frac{\nu_k^2}{\sigma^2}\right), \tag{13}$$

where $f(\alpha, \dot{\alpha})$ is the joint PDF of the signal envelop α and its time deviation $\dot{\alpha}$ [41], and f_D denotes the maximum Doppler frequency shift. For the assumed slow-varying fading channels, the channel state will remain invariant in each frame duration T_F. Correspondingly, the average number of static sensing slots, under the k_1th representative state, can be estimated by $R_{k_1} = \pi_{k_1}/T_F$. Thus, the transitional probability may be approximated by the ratio of the expected occurrence times of state-crossing (i.e., N_{k_2}) and the average number of discrete states (i.e., R_{k_1}), i.e., $\Pi_{k_1\to k_2} \backsimeq N_{k_2}/R_{k_1}$. Although this transitional probability $\Pi_{k_1\to k_2}$ is derived numerically from a rough *dimensional* analysis, its applicability has been verified [28], which is also widely used in literatures [36]–[38], [42]. Note that, the above analysis may be naturally generalized to other cases, e.g., Rician and Nakagami distributions.

C. Observation

For the ease of implementations, ED has been widely recommended as a fundamental technique for spectrum sensing. This work will establish a general model based on ED. Before

$$\boldsymbol{\Pi}_{K\times K} = \begin{bmatrix} \Pi_{0\to0} & \Pi_{1\to2} & 0 & 0 & \cdots & 0 & 0 & 0 \\ \Pi_{1\to0} & \Pi_{1\to1} & \Pi_{1\to2} & 0 & \cdots & 0 & 0 & 0 \\ \vdots & \vdots & \vdots & \vdots & \ddots & \vdots & \vdots & \vdots \\ 0 & 0 & 0 & 0 & \cdots & \Pi_{(K-2)\to(K-3)} & \Pi_{(K-2)\to(K-2)} & \Pi_{(K-2)\to(K-1)} \\ 0 & 0 & 0 & 0 & \cdots & 0 & \Pi_{(K-1)\to(K-2)} & \Pi_{(K-1)\to(K-1)} \end{bmatrix} \tag{12}$$

proceeding, it is necessary to briefly illustrate the ED method, which is formulated to the following two hypotheses [5]

$$y_n = \begin{cases} \sum_{m=1}^{M} z_{n,m}^2 & H_0 \quad (14a) \\ \sum_{m=1}^{M} (\alpha_n u_{n,m} + z_{n,m})^2 & H_1 \quad (14b) \end{cases}$$

where $M = T_S \times f_s$ is the length of samples, and f_s is the sampling frequency. H_0 and H_1 denote the two hypotheses corresponding to the absence and presence of PU signals (i.e., S_0 and S_1), respectively; y_n is the summed energy in SUs receiver; $u_{n,m} = s_{n,m} b_{n,\lfloor m/N_s \rfloor} \times \tilde{p}(m - N_s/2)$ is the received baseband signal of the nth sensing slot, where $\{b_{n,m}\}$ denote the PU's information symbols, $\tilde{p}(m - N_s/2)(m = 0, 1, \ldots, N_s)$ is the periodic pulse-shaping response and N_s is its periodic length. For simplicity, the real-valued BPSK signal is considered, e.g., $b_{n,m} \in \{+1, -1\}$. The additive white Gaussian noise (AWGN) noise is $z_{n,m}$, with a variance of σ_z^2. As noted from the algorithm derivations, the extension to the complex signal and noise model (e.g., M-PSK and M-QAM) is straightforward (see the Appendix for details).

In realization, a band-pass filter is adopted to collect the frequency components of interest. Given the channel state α_n, the likelihood function $p(y_n|\alpha_n, s_{n,m})$ follows conditionally a central chi-square distribution with M degrees of freedom (DoF) under H_0, and a non-central chi-square distribution with M degrees under H_1, i.e.

$$p(y_n|\alpha_n, s_{n,m} = 0) \sim \chi_M^2, \quad (15a)$$

$$p(y_n|\alpha_n, s_{n,m} = 1) \sim \chi_M^2(\kappa), \quad (15b)$$

where $\kappa = \sum_{m=1}^{M} |\alpha_n u_{n,m}|^2$ denotes the noncentral parameter, which is related with the time-dependent fading gain α_n and the average power of PU signals.

For traditional ED, a decision threshold τ could be properly determined based on certain criterions. Then, the false alarm probability P_f is defined as $P(y_n > \tau|H_0)$, while the detection probability P_d is $P(y_n > \tau|H_1)$.

$$P_f \triangleq \Pr(H_1|H_0) = \frac{\Gamma(M, \tau/2)}{\Gamma(M/2)}, \quad (16a)$$

$$P_d \triangleq \Pr(H_1|H_1) = Q_M(\sqrt{2\gamma}, \sqrt{\tau}), \quad (16b)$$

where $\gamma = \alpha_n^2 \sigma_u^2 / \sigma_z^2$ is the instantaneous SNR at the nth sensing slot, and σ_u^2 is the variance of PU signals. $\Gamma(a, x) = \int_x^\infty t^{a-1} \exp(-t) dt$ is the incomplete gamma function, and $\Gamma(a)$ denotes the gamma function. $Q_{M/2}(a, x)$ is the generalized Marcum Q-function which is given by $Q_{M/2}(a, x) = (1/a^{M/2-1}) \int_x^\infty t_{M/2} \exp(-(t^2 + a^2/2)) I_{M/2-1}(at) dt$, where $I_{M/2-1}(\cdot)$ is the modified Bessel function of the first kind and order $M/2 - 1$. Accordingly, the missed probability $P_m \triangleq \Pr(H_0|H_1)$ is given by $1 - P_d$.

Notice that, in realistic CR networks, P_f and P_d may have quite different negative effects. False alarms would prevent the unused spectral segments from being accessed by SUs, so a high P_f implies a low spectral utilization. The missed detections measure the interferences from SUs to PU, which should be limited in realistic scenarios. Thus, the main metric of sensing performance is either to minimize P_m for a target P_f, or to minimize P_f with a target P_m. Based on an overall consideration of the spectral utilization of unused bands and the potential interference to PUs, in this investigation we focus mainly on the total error detecting probability [23], [43], which is specified by $\Omega = P_m P(H_1) + P_f P(H_0)$. Correspondingly, for the threshold-based classical ED which fails to exploit the time-variation of fading gains unfortunately and can only utilizing its static PDF, the optimal threshold may be determined from

$$\tau_{ED} = \arg\max_{\tau} \left\{ 1 - \frac{\lambda}{\mu + \lambda} - \frac{\mu}{\mu + \lambda} \times P_f(\tau) + \frac{\lambda}{\mu + \lambda} \times P_{d,Rayleigh}(\tau) \right\}, \quad (17)$$

where $P_{d,Rayleigh}(\tau)$ is the detection probability of non-mobile Rayleigh fading channels [25].

D. DSM of Spectrum Sensing in TVFF

Based on the elaborations above, we may now formulate the DSM of spectrum sensing in the considered TVFF channels, as is in (18)–(20).

$$s_n = F(s_{n-1}) \quad (18)$$

$$\alpha_n = H(\alpha_{n-1}) \quad (19)$$

$$y_n = G(\alpha_n, s_{n,m}, z_{n,m}) \quad (20)$$

In the formulated DSM, two hidden states, i.e., $s_{n,m}$ and α_n, evolves independently according to the *dynamic equations* $F(\cdot)$ and $H(\cdot)$, respectively, which are non-analytical due to stochastic transitions in eq. (4) and (12). In practice, the mapping relationships of $F(\cdot)$ and $H(\cdot)$ will be determined probabilistically by the *a priori* transitional properties. The observation is obtained from the nonlinear and noisy *measurement equation* $G(\cdot)$ in eq. (20). For convenience, three important aspects are assumed in the formulated DSM.

1) The TVFF channel gain α_n is assumed to be invariant (or steady) within several successive sensing slots. The ratio of the lasting duration of α_n and the number of sensing periods T_F, which is denoted by L, is practically associated with the maximum Doppler frequency shift f_D [43]. To be specific, a larger $f_D \propto (1/LT_F)$ leads to a smaller L.
2) The discrete state of fading gain α_n is assumed to evolve at the exact edge of the sensing slot $n' = \lfloor n/L \rfloor$, so that we deal with a constant α_n within each slot. Despite for the analysis simplicity, such a presumption may also become practically valid for the slow varying channel (i.e., $T_S \ll (1/f_D)$).
3) The PU's state keeps invariant during each sensing slot, i.e., $s_{n,m} = s_n$. Thus, the statistical property of PU signals $u_{n,m}$ will not be changed.

III. Joint Estimation

As far as the established DSM is concerned, SUs may become blind as no information could be obtained from PUs, except for the radio energy in nearby environments. In order to deal with fading effects, classical energy-based sensing schemes have to use the marginalization or collaborative techniques, which unfortunately ignores the time-variation of realistic channels. These methods, therefore, may become less competitive in TVFF channels. In contrast, in the new designed sensing algorithm, both the fading gain α_n and the primary state s_n will be estimated jointly.

From a Bayesian point of view, the joint estimations of the PU state and the dynamic fading channel can be derived by maximizing the posterior probability $p(\alpha_{0:n}, s_{0:n}|y_{0:n})$, i.e.,

$$(\hat{\alpha}_n, \hat{s}_n) = \arg \max_{\alpha_n \in \mathbb{A}, s_n \in \mathbb{S}} p(\alpha_n, s_n|y_n)|p(\alpha_n|\alpha_{n-1}), p(s_n|s_{n-1}). \tag{21}$$

Here, $y_{0:n} \triangleq \{y_0, y_1, \ldots, y_n\}$ accounts for the observation trajectory till the nth sensing time slot. Similarly, $\alpha_{0:n}$ and $s_{0:n}$ denote the trajectories of two hidden states, respectively. With the derived MAP estimations, as has been indicated, one significant performance metric of the new threshold-free scheme is the probability of detections, which is given by $P_D := 1 - \Omega = 1 - p(H_1) - (\mu/\mu + \lambda) \times P_f + (\lambda/\mu + \lambda) \times P_d$.

A. Sequential MAP Detection

Given two independent hidden Markov states (α_n and s_n) and independent noise samples assumed in this investigation, we may have

$$\begin{aligned} &p(\alpha_{0:n}, s_{0:n}|y_{0:n}) \\ &\quad \propto p(\alpha_0, s_0) \times \prod_{i=1}^{n} p(y_i|\alpha_i, s_i) p\left[(\alpha_i, s_i)|(\alpha_{i-1}, s_{i-1})\right] \\ &\quad \overset{(a)}{=} p(\alpha_0)p(s_0) \times \prod_{i=1}^{n} p(y_i|\alpha_i, s_i)p(\alpha_i|\alpha_{i-1})p(s_i|s_{i-1}), \end{aligned} \tag{22}$$

where (a) holds due to the considered data-independent FSMC model, and thus we have $p(\alpha_0, s_0) = p(\alpha_0)p(s_0)$ and $p[(\alpha_i, s_i)|(\alpha_{i-1}, s_{i-1})] = p(\alpha_i|\alpha_{i-1})p(s_i|s_{i-1})$.

According to the alternating renewal process, the transitional probability $p(s_i|s_{i-1})$ is time-varying and non-stationary, which is actually related with the lasting intervals (i.e., q) of current state. For clarity, we may denote it by $p_{i,q}(s_i|s_j, s_{j\in[i-q+1,i-1]} = 1 \oplus s_{i-q})$, where $1 \oplus s_{i-q}$ accounts for the complementary state of s_{i-q}. Furthermore, taking the slow time-varying fading gain into account (i.e., with a minimum residence time equal to L sensing slots), we may rewritten the joint *a posteriori* probability to eq. (23), shown at the bottom of the page.

Noted from eq. (23) that the evolution of fading gain will remain asynchronous with that of PU states, which may be in collusion with the non-stationary property and, therefore, pose great challenges to joint estimations in the considered new sensing scenarios. Meanwhile, in CR networks, it is desirable to evaluate the posterior probability and accomplish spectrum sensing in time as the new observation arrives.

The recurrence estimation is considered as a promising way to tackle above difficulties, which sequentially updates the involved posterior probability by incorporating the new information of observations. Following the well-known Chapman–Kolmogorov equation and the Markov process of order one, we may further update $p(\alpha_{0:n}, s_{0:n}|y_{0:n})$ recursively by eq. (24), also shown at the bottom of the page.

Unfortunately, attributed to the intractable marginalization, the time-dependent dynamics of the specific problem as well as the intermittent disappearance of the likelihood density of fading gains (e.g., in the case of H_0), usually the posterior distribution of interest cannot be determined analytically in practice. Thus, the above recurrence update could only be considered as a theoretical (or conceptional) Bayesian statistical inference.

B. Particle Filtering

As a feasible approach that may avoid intractable computations and cope with complex distributions effectively, the sequential importance sampling inspired PF shows great promise to the joint estimations-based spectrum sensing in TVFF channels. Relying on a simulated Monte-Carlo method and the numerical approximation technique, SIS could obtain the consistent estimation of the posterior probability via a group of discrete random measures (i.e., particles) $x^{(i)}$ with different probability masses (or weights) $w^{(i)} (i = 1, 2, \ldots, I)$, where I is the size of particles [29], [44].

With PF, the random particles are firstly simulated from an unknown distribution related with the target probability $p(x)$. Then, the continuous distribution $p(x)$ is approximated numerically by

$$p(x) = \sum_{i=1}^{I} w^{(i)} \delta\left(x - x^{(i)}\right), \tag{25}$$

where $\delta(x)$ is the Dirac delta function. Based on (25), the expectation of any associated arbitrary features of x, i.e.,

$$p(\alpha_{0:n}, s_{0:n}|y_{0:n}) \propto p(\alpha_0)p(s_0) \times \prod_{i=1}^{n} p(y_i|\alpha_i, s_i) p\left(\alpha_{\lfloor i/L \rfloor}|\alpha_{\lfloor i/L \rfloor - 1}\right) p_{i,q}\left(s_i|s_{i-1}, s_{j\in[i-q+1,i-1]} = 1 \oplus s_{i-q}\right) \tag{23}$$

$$p(\alpha_{0:n}, s_{0:n}|y_{0:n}) = p(\alpha_{0:n-1}, s_{0:n-1}|y_{0:n-1}) \times \frac{p(y_n|\alpha_n, s_n)p(\alpha_n|\alpha_{n-1})p(s_n|s_{n-1})}{\int\int_{\alpha_n \in \mathbb{A}, s_n \in \mathbb{S}} p(y_n|\alpha_n, s_n)p(\alpha_n, s_n|y_{0:n-1})d\alpha_n ds_n} \tag{24}$$

$\mathbb{E}(g) = \int_{x_{0:n}} g(x_{0:n}) p(x_{0:n}|y_{0:n}) dx_{0:n}$, may be then effectively evaluated via $\hat{\mathbb{E}}(g) = \sum_{i=1}^{I} g(x^{(i)}) w^{(i)}$ when $I \to \infty$.

To accomplish this, two steps are involved in PF, i.e., (1) draw the particles $x_n^{(i)}$ by sampling the importance distribution, and (2) update the associated weight $w_n^{(i)}$.

1) Draw Particles: For most realistic applications, it is infeasible to sample from the target posterior distribution $p(x)$ directly. To obtain these discrete measures, an importance distribution function $\pi(x_n|x_{0:n-1}^{(i)}, y_{0:n})$ is designed, from which discrete particles can be drawn conveniently, i.e., $x^{(i)} \sim \pi(x_n|x_{0:n-1}^{(i)}, y_{0:n})$. Thus, the importance function $\pi(x_n|x_{0:n-1}^{(i)}, y_{0:n})$ is supposed to be related closely with the target posterior distribution and may have a significant impact on the estimation performance [29], [44], which should be carefully designed in accordance with realistic situations.

In practice, two kinds of importance distributions are recommended usually, i.e., the prior and the optimal importance function. The prior importance function is chosen as $p(x_n|x_{n-1}^{(i)})$, which is easy to implement but can hardly exploit the involved information in observations (i.e., y_n). The optimal importance function, which can minimize the one-step variance of the importance weights and hence promote the effectiveness of particles estimation, is given by $p(x_n|x_{0:n-1}^{(i)}, y_{0:n})$. In the following analysis, the optimal importance function will be adopted and, correspondingly, the new particles $x_k^{(i)} (i = 1, 2, \ldots, I)$ are drawn by simulating random variables from $p(x_n|x_{0:n-1}^{(i)}, y_{0:n})$.

2) Update Weights: In order to approximate $p(x_n|y_{0:n})$, the associated weights $w^{(i)}$ are updated by

$$w^{(i)} = p(x_n|y_{0:n}) / \pi\left(x_n|x_{0:n-1}^{(i)}, y_{0:n}\right). \tag{26}$$

Given that the specified importance function may be usually factored as

$$\pi(x_{0:n}|y_{0:n}) = \pi(x_n|x_{0:n-1}, y_{0:n}) \pi(x_{0:n-1}|y_{0:n-1}), \tag{27}$$

then the updating of importance weights $w_n^{(i)}$ can be written as [29], [44]

$$w_n^{(i)} \propto \frac{p\left(y_n|x_n^{(i)}\right) p\left(x_n^{(i)}|x_{n-1}^{(i)}\right)}{\pi\left(x_n^{(i)}|x_{0:n-1}^{(i)}, y_{0:n}\right)} w_{n-1}^{(i)}. \tag{28}$$

As far as the assumed optimal importance distribution is concerned, the importance weight $w^{(i)}$ may be further propagated recursively via

$$w_n^{(i)} \propto p\left(y_n|x_{n-1}^{(i)}\right) \times w_{n-1}^{(i)}. \tag{29}$$

As the approximation of one realistic probability distribution, the importance weights should further be normalized to 1, i.e., $w^{*(i)} = w^{(i)} / \sum_{i=1}^{M} w^{(i)}$. Notice that, some particle weights may become negligible as the sequential estimation proceeds, resulting in inefficient estimations. In order to deal with the degeneration of particle weights, a resample procedure is also necessary to eliminate some negligible particles and thereby improve the estimation performance [29].

C. Joint Estimation Based Spectrum Sensing

In this section, we will design a promising sensing scheme for TVFF scenarios, which can estimate the fading gain and unknown PU state jointly. In sharp contrast to joint detections in classical communication systems, where the information of channel coefficients is always enclosed in received signals, unfortunately the fading gain α_n will be disappeared completely from the observation y_n when the PU state is "0". This particular feature may present a difficult puzzle to the practical design of joint estimations.

To meet the challenges posed by this specific problem, we develop a recursive algorithm which could modify the estimations of fading gain and PU state successively. The proposed algorithm contains three steps, i.e., (1) a coarse detection used to identify the rough (inaccurate) PU state, (2) the statistical estimation of fading gain, and (3) PF-based PU state estimation. To be specific, the Step (1) is firstly applied to obtain a rough perception of unknown PU state. If there is no PU signal or the observation involves nothing about the fading channels, then only the *a priori* TPM will be utilized to identify the most probable fading state of the current slot, with the help of the estimated state of the last slot. Otherwise, the MAP estimation of α_n will be derived. Subsequently, Steps (2) and (3) will be executed iteratively in order to further refine the estimations of two hidden states (i.e., $\hat{\alpha}_n$ and $\hat{s}_n$). Thus, the iterative scheme may realize joint estimations even when the fading gain become disappeared in the case of $s_n = 0$.

1) Coarse Detection: As the information involved by observations may vary dramatically with different PU states, the coarse detection procedure is designed to obtain a rough estimation of unknown PU state. On this basis, subsequent estimation methodologies for fading channel can be then determined. To accomplish this, we may specify a threshold by

$$\tau_{CD} = M \times \left[B^2 \sigma_u^2 \times \mathbb{E}\left(\alpha_n^2\right) + \sigma_z^2\right], \tag{30}$$

where B^2 denote the average power of PU signals, which may be usually normalized to 1 without losing generality. Thus, the threshold is associated with the samples size M, the expected fading gain $\mathbb{E}(\alpha_n^2) \triangleq \sum_{k=0}^{K-1} \alpha_k^2 \pi_k$ as well as the noise variance σ_z^2. Relying on the rough threshold, the initial estimation on PU state, denoted by i_n, is derived by

$$i_n = \begin{cases} 1 & \tau_{CD} \le y_n, \quad (31a) \\ 0 & \tau_{CD} > y_n. \quad (31b) \end{cases}$$

2) Estimation of Fading Gain: As mentioned, the estimation strategy for fading gains relies heavily on different initial estimations of PU states based on two practical considerations. First, the likelihood information is unavailable in the absence of PU signals (i.e., $s_n = 0$). In such a case, the MAP estimation of fading gain may become infeasible and, consequently, only the prior TPM can be utilized to update α_n. Second, for the slow time-varying channel with its dynamic amplitude remaining invariant in several sensing periods temporarily, the estimated fading gain can be further refined by fully utilizing historical observations in the case of $s_n = 1$. Therefore, the designed sensing algorithm is *event-triggered* (i.e., initial PU state) and *information-driven* (i.e., historical observations).

(1) If we have $i_n = 0$, then there is little innovation information can be utilized in the sensing slot n' in which state transitions of fading gains may occur, i.e., $n' = \lfloor n/L \rfloor$, expect for the *a priori* transitional probability. In such a case, we may directly obtain the estimation of α_n by using

$$\hat{\alpha}_{n'} = \arg \max_{\alpha_{n'} \in \mathbb{A}} p\left(\alpha_{n'} | \hat{\alpha}_{n'-1}\right). \tag{32}$$

In the other remaining slots $n = (n' + l)(1 \le l < L)$, the fading gain will be assumed to be unchanged, i.e., we have $\hat{\alpha}_{n'+l} = \hat{\alpha}_{n'}$.

(2) If we have $i_n = 1$, then in the sensing slot $n' = \lfloor n/L \rfloor$ in which the transition of fading gain may occur, the observation (i.e., the summed energy) and the related likelihood could be fully exploited. Thus, we may obtain the estimation of fading gain by maximizing the *a posteriori* probability

$$\begin{aligned} \hat{\alpha}_{n'} &= \arg \max_{\alpha_{n'} \in \mathbb{A}} p(\alpha_{n'} | y_{n'}, i_{n'} = 1, \hat{\alpha}_{n'-1}) \\ &= \arg \max_{\alpha_{n'} \in \mathbb{A}} p(y_{n'} | \alpha_{n'}, i_{n'} = 1) p(\alpha_{n'} | \hat{\alpha}_{n'-L}). \end{aligned} \tag{33}$$

The likelihood term in eq. (33) follows a non-central chi-square distribution with M DoF theoretically, conditional on the estimated initial PU state $i_{n'} = 1$. Thus, we may have:

$$p(y_{n'} | \alpha_{n'}, i_{n'} = 1) \sim \chi^2_M(\kappa_0), \tag{34}$$

where $\kappa_0 = \sum_{m=1}^{M} |\hat{\alpha}_{n'} u_{n',m}|^2$ denotes the noncentral parameter which may be associated with the estimated fading channel gain.

Then, in the following slots $n = (n' + l)(1 \le l < L)$, we may make full use of the past observations to further modify the estimation of fading gains. More specifically, in subsequent slots, based on the historical information we may redefine an accumulated observation $y_{n,l}$ by

$$y_{n,l} = \sum_{m=1}^{M} \alpha_{n'} u_{n,m} + z_{n,m})^2 + \sum_{l_n=1}^{l-1} y_{n',l_n}. \tag{35}$$

It is expected from eq. (35) that, with more information from observations exploited, the estimation of fading gain will become more accurate. Notice that, such an accumulated observation $y_{n,l}$ $(1 \le l < L)$ also follows the non-central chi-square distribution, but with the accumulated degree increased to Ml, i.e.,

$$p(y_{n,l} | \alpha_{n'}, i_n = 1) \sim \chi^2_{Ml}(\kappa_l) \tag{36}$$

where the noncentral parameter is $\kappa_l = \sum_{m=1}^{M(l+1)} |\hat{\alpha}_{n'} u_{n,m}|^2$.

3) Particle Filtering Based PU State Estimation: Although an initial estimation of PU state (i.e., i_n) has be derived during the first stage (i.e., coarse detection), such a rough estimation unfortunately ignores the time-varying fading gain and, therefore, may usually become inaccurate. Thus, in our iteratively implemented sensing scheme, after the sequential computation of fading gain, the PU state will be further modified recursively based on PF. Notice that, such an estimated PU state, which is treated as a soft-output, will be employed subsequently by Step (2) to further revise the fading gain. After the total R times of successive refinement of fading gain $\hat{\alpha}_n$ and PU state $\hat{s}_n$, the final estimation of PU state will be derived.

Within an SIS processing framework, the *a posteriori* probability is numerically updated in time via a group of updated particles $x^{(i)}_{0:n}$ and the associative weights $w^{(i)}_{0:n}$ $(i = 0, 1, 2, \ldots, I-1)$. In the nth sensing slot, the innovation information carried by the new observation y_n can be incorporated effectively with the historical knowledge. Thus, the Bayesian statistical inference can be accomplished properly and, consequently, the PU state can be estimated by maximizing the approximated posterior density.

In practice, after updating the fading gain, building on the new observation y_n we may derive the new particles from the importance distribution, i.e., $x^{(i)}_n \sim \pi(x_n | x^{(i)}_{0:n-1}, \hat{\alpha}_{n'}, y_n)$. In this investigation, the optimal importance distribution is specified by

$$\begin{aligned} &\pi\left(x_n | x^{(i)}_{0:n-1}, \hat{\alpha}_{n'}, y_n\right) \triangleq p\left(x_n | x^{(i)}_{0:n-1}, \hat{\alpha}_{n'}, y_n\right) \\ &= p(y_n | \hat{\alpha}_{n'}, x_n) p_{n,q}\left(x_n | x^{(i)}_{n-j}, x_{j \in [n-q+1, n-1]} = 1 \oplus x_{n-q}\right) \end{aligned} \tag{37}$$

After sampling from the importance distribution, the associated weights (i.e., the probability pass of new particles) should be updated accordingly. For the optimal importance distribution, particle weights should be recursively updated by

$$w^{(i)}_n = w^{(i)}_{n-1} \times p(y_n | x^{(i)}_{n-1}, \hat{\alpha}_n). \tag{38}$$

The likelihood term in eq. (38), conditioned on the estimated fading gain and the past derived particles $x^{(i)}_{n-1}$, can be given by eqs. (39) and (40), shown at the bottom of the page. $\lambda = M\hat{\alpha}^2_{n'} / (\sigma^2_u + \sigma^2_z)$.

$$\begin{aligned} p\left(y_n | \hat{\alpha}_n, x_{n-1} = 0\right) &\propto p(y_n | \hat{\alpha}_n, x_n = 0) p\left(x_n = 0 | x^{(i)}_{n-1} = 0\right) + p(y_n | \hat{\alpha}_n, x_n = 1) p\left(x_n = 1 | x^{(i)}_{n-1} = 0\right) \\ &= \frac{1}{2^{M/2} \Gamma(M/2)} y_n^{M/2-1} \exp\left(-\frac{y_n}{2}\right) \times p_{00}(q) + \left(\frac{y_n}{\lambda}\right)^{\frac{M-2}{4}} \exp\left(-\frac{y_n + \lambda}{2}\right) I_{\frac{M}{2}-1}(\sqrt{\lambda y_n}) \times [1 - p_{00}(q)], \end{aligned} \tag{39}$$

$$\begin{aligned} p(y_n | \hat{\alpha}_n, x_{n-1} = 1) &\propto p(y_n | x_n = 1, \hat{\alpha}_n) p\left(x_n = 1 | x^{(i)}_{n-1} = 1\right) + p(y_n | x_n = 0, \hat{\alpha}_n) p\left(x_n = 0 | x^{(i)}_{n-1} = 1\right) \\ &= \left(\frac{y_n}{\lambda}\right)^{\frac{M-2}{4}} \exp\left(-\frac{y_n + \lambda}{2}\right) I_{\frac{M}{2}-1}(\sqrt{\lambda y_n}) \times p_{11}(q) + \frac{1}{2^{M/2} \Gamma(M/2)} y_n^{M/2-1} \exp\left(-\frac{y_n}{2}\right) \times [1 - p_{11}(q)] \end{aligned} \tag{40}$$

Based on the new derived particles and the associated weights, we may finally obtain the estimation of PU state by using the asymptotical MAP criterion in eq. (41), if the particles size I is sufficiently large.

$$\hat{s}_n = \max_{s_n \in \mathbb{S}} p(s_n | y_{0:n}, s_{0:n-1}, \hat{\alpha}_{n'}), \tag{41}$$

where the *a posteriori* density can be numerically approximated by using eqs. (42) and (43).

$$p(s_n = 0 | y_{0:n}, s_{0:n-1}, \hat{\alpha}_{n'}) \simeq p\left(s_n = 0 | y_{0:n}, s_{0:n-1}^{(i)}, \hat{\alpha}_{n'}\right) = \frac{\sum_{i \in \mathbb{X}_0} w_n^{(i)}}{\sum_{i=1}^{I} w_n^{(i)}}, \mathbb{X}_0 = \left\{ i | x_n^{(i)} = 0 \right\}, \tag{42}$$

$$p(s_n = 1 | y_{0:n}, s_{0:n-1}, \hat{\alpha}_{n'}) \simeq p\left(s_n = 1 | y_{0:n}, s_{0:n-1}^{(i)}, \hat{\alpha}_{n'}\right) = \frac{\sum_{i \in \mathbb{X}_1} w_n^{(i)}}{\sum_{i=1}^{I} w_n^{(i)}}, \mathbb{X}_1 = \left\{ i | x_n^{(i)} = 1 \right\}. \tag{43}$$

D. Implementations

Based on the elaborations above, the implementation flow of the proposed sensing algorithm, which jointly estimates the fading gain and PU state based on a formulated DSM, is plotted in Fig. 2.

- Step 1: Based on the current observation y_n, the coarse detection is conducted. Thus, the initial estimation of PU state (i.e., i_n) would be obtained from eq. (31), by comparing y_n with τ_{CD}.
- Step 2: Depending on different i_n, the fading gain is updated. In specific, in the case of $i_n = 1$, the channel amplitude is estimated by maximizing the *a posteriori* probability as in eq. (33), and, if possible, by also integrating the historical information (i.e., $y_{n':n}$); while for $i_n = 0$, only the *a priori* transitional probability can be utilized as in eq. (32).
- Step 3: Based on the Bayesian sequential detection, the PU state is derived by using an SIS approach. In this process, presumed on the estimated fading gain, the posterior probability of PU state is approximated numerically via I discrete particles with evolving weights as in eqs. (41)–(44). Subsequently, the estimated PU state will be further employed by *Step 2* (i.e., $i_n = \hat{s}_n$) to iteratively refine $\hat{\alpha}_n$.

From the schematic algorithm flow, it is worth noting that there may contain two counters in this proposed spectrum sensing algorithm.

1) The first counter l is mainly concerned with the second phase, i.e., the MAP estimation of fading gain. Such a counter is reset to 0 each time the state transition of fading gain occurs. Then, as the increasing of the sensing slot index, the counter l is also increased to record the number of accumulated observations, which is of great importance to determine the DoF of the accumulated observation $y_{n,l}$. More specifically, after the evaluation of $y_{n,l}$ and the refinement of fading gain, the counter l should be updated by $l = l + 1$.

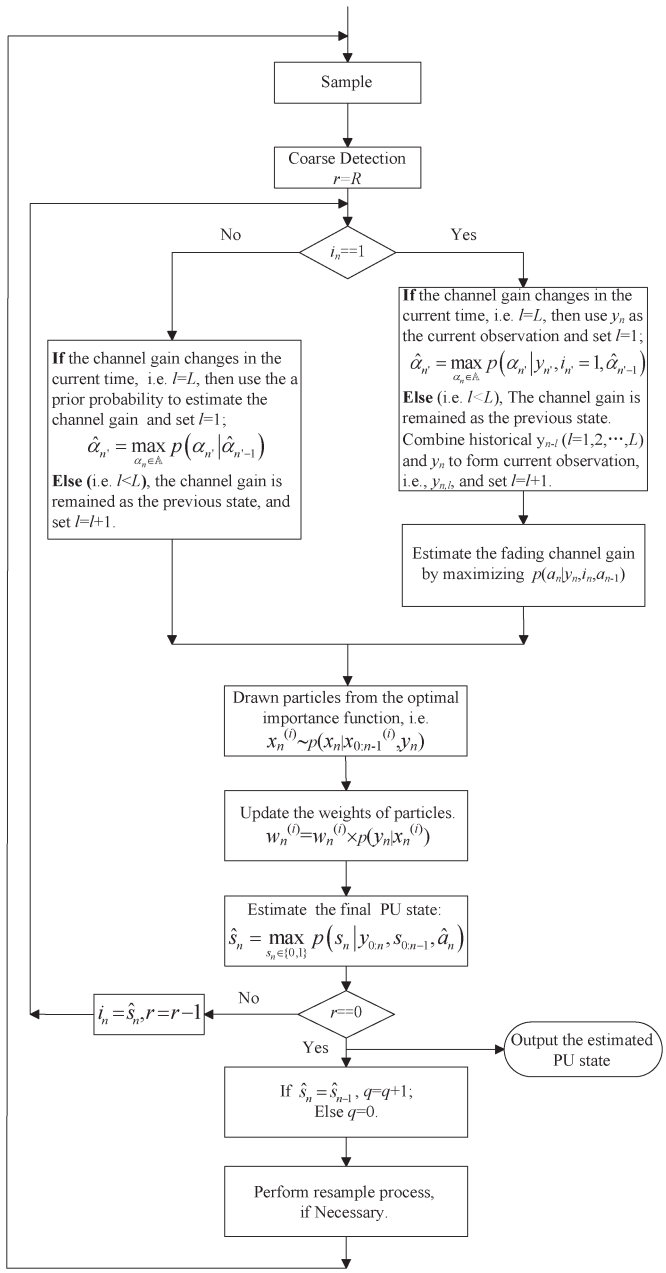

Fig. 2. Algorithm flow of the proposed joint estimation based spectrum sensing algorithm for TVFF channels.

2) The second counter q is used by the third phase, i.e., the PF-based PU state estimation. Since the *a priori* state transitional probability is practically related the lasting slots q of the current state, another counter is required to dynamically determine the state transition probability in subsequent slots. If $\hat{s}_n = \hat{s}_{n-1}$, this counter will be updated by $q = q + 1$; and otherwise, it will be reset to $q = 0$.

E. Complexity

The complexity of the presented algorithm mainly involves the following three parts. For the first stage (i.e., *Coarse Detection*), the number of multiplications in calculating y_n is $\mathcal{O}(M)$. Then, during the second phase (i.e., *Estimation of Fading*

Gain), given the K-state FSMC model, the estimation of fading gain has to exhaustively evaluate the total K possible transitional probabilities. Taking the 1st order FSMC model into account, the number of feasible transitional states will decrease to $K_1 = 3$. Given the computations of likelihood distributions, the complexity is thereby measured by $\mathcal{O}[K_1 \times \mathcal{K}(n_b)]$, where n_b is the number of digital-bits of precision. In order to evaluate the involved mathematical functions (e.g., the Gamma function), in practice we may have $\mathcal{K}(n_b) \propto (\log(n_b))^2$ [45]. For the third stage (i.e., *PU State Estimation*), the numbers of involved multiplications will become proportional to the adopted particle size I and, therefore, the complexity is measured by $\mathcal{O}[I \times \mathcal{K}(n_b)]$. Further considering multiple iterations R, the complexity of the proposed algorithm, which may be measured roughly by the total numbers of multiplications, is given by $\mathcal{O}[M + R \times (K_1 + I) \times \mathcal{K}(n_b)]$. In contrast, the traditional ED has a lower complexity of $\mathcal{O}(M)$. Another widely used sensing scheme, known as the covariance absolute value (CAV) detection, has a complexity of $\mathcal{O}(K_a M + K_a^2)$ [16], where K_a accounts for the smoothing factor $(10 < K_a < 15)$. When the sampling size M is large, we have $(K_a \times M) > [M + R \times (K_1 + I) \times \mathcal{K}(n_b)] > M$, i.e., the new method is slightly more complex than ED while less complex than the CAV scheme.

IV. Numerical Simulations and Performance Evaluations

In this section, we will evaluate the presented new algorithm in realistic TVFF channels. ED is used for comparative analysis since the summer-energy is adopted by our new DSM and estimation process.

A. Iteration Number R

We firstly evaluate the performance with different numbers of iterations (i.e., R). In the simulation, the samples size M is set 10, the transitional rates (λ, μ) are configured to $((1/10T_F), (1/5T_F))$, the static duration L is 50 and the representative partitioned number of TVFF is $K = 5$. We note from Fig. 3 that such an iterative scheme may noticeably improve the sensing performance. Specifically, an SNR gain of 3 dB can be archived in high SNRs by using 3 iterations. However, noted from the complexity analysis, further more iterations (e.g., $R = 4$) proved of little avail, but with a significantly increased complexity. Thus, $R = 3$ can be suggested to enhance performance while also maintaining an affordable complexity.

B. Particle Size I

This second experiment is devoted to evaluating the performance under different particle size (i.e., I). In the simulation, the samples size M is set 10, (λ, μ) are configured to $((1/10T_F), (1/5T_F))$, the static duration L is 50 and the representative partitioned number of TVFF is $K = 5$. We may note from Fig. 4 that, with the increasing of the number of random particles, the sensing performance may be enhanced. For example, a detection gain of 1.8 dB may be acquired in high SNRs region, when I is increased from 3 to 20.

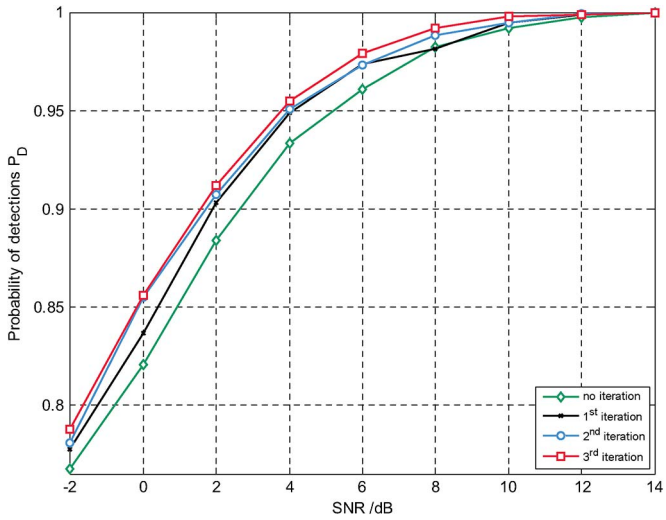

Fig. 3. Sensing performance of the presented joint estimation algorithm under different iteration number R. Notice that, $K = 5$, $M = 10$, $L = 50$, and $(\lambda, \mu) = ((1/10T_F), (1/5T_F))$.

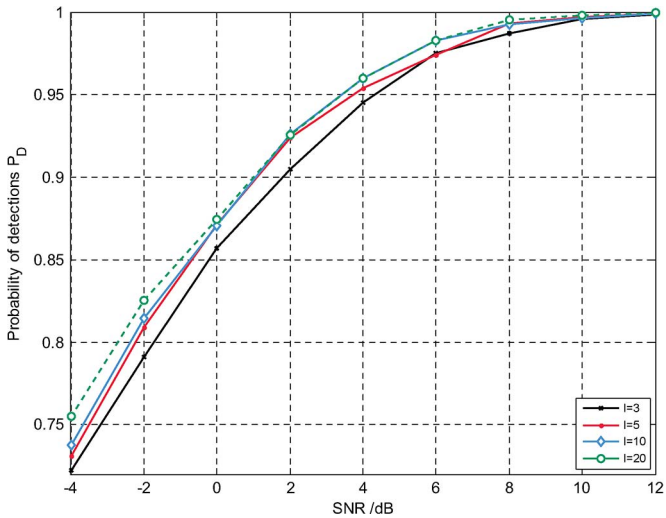

Fig. 4. Sensing performance of the presented joint estimation algorithm under different particle size I. Notice that, $K = 5$, $M = 10$, $L = 50$, and $(\lambda, \mu) = ((1/10T_F), (1/5T_F))$.

C. Representative State K

We may now investigate the influence from the partitioning levels of fading gains (i.e., K). In this experimental simulation, we configure the static slots duration L to 20, the transitional rates (λ, μ) to $((1/10T_F), (1/5T_F))$ and the sample size M to 10.

In practice, K may be configured to $2 \sim 1000$. Notice that, however, a compromise between the representative accuracy and the implementation complexity should be made in practical designs. That is, the larger K is, the more accurate the FSMC model is, yet the higher the complexity is. As suggested, a partitioning size of $K \geq 8$ may be usually sufficient for most realistic applications [33]. As far as this specific problem is concerned, such a parameter may have an insignificant impact on the sensing performance. As demonstrated by numerical results in Fig. 5, the performances with $K = 5, 8, 10$ are basically comparable. The reason is easy to follow, i.e., with the proposed

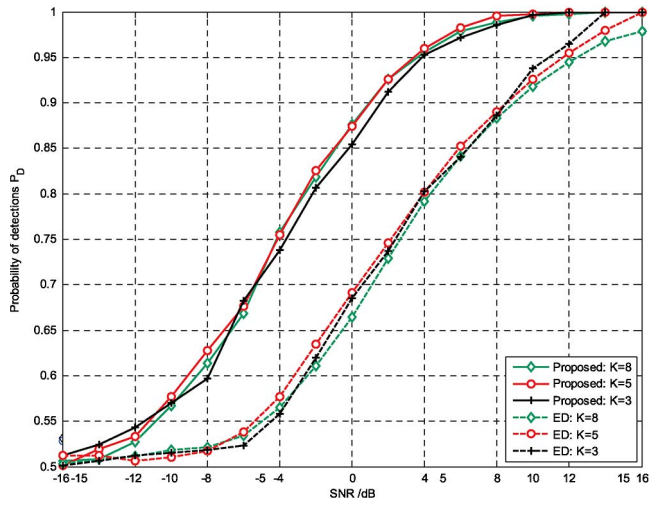

Fig. 5. Sensing performance of the presented joint estimation algorithm under different K. Notice that, $M=10$, $L=20$, and $(\lambda,\mu)=((1/10T_F),(1/5T_F))$.

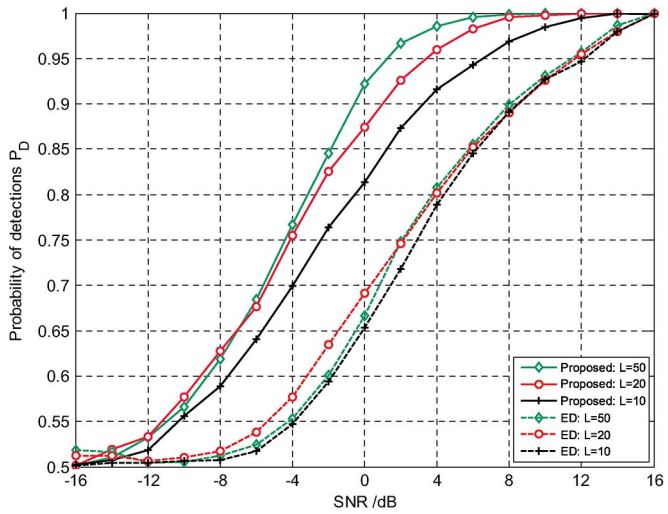

Fig. 6. Sensing performance of the presented joint estimation algorithm under different L. Notice that, $K=5$, $M=10$, and $(\lambda,\mu)=((1/10T_F),(1/5T_F))$.

DSM-based sensing algorithm, the fading gain could be estimated jointly in time. So, even with quite different partition numbers (i.e., $5\sim10$), the overall estimation errors (especially for the sensing performance) would be affected insignificantly. Therefore, in the following experimental demonstrations, K may be configured to 5.

D. Doppler Frequency Shift f_D

As an indicator of the changing rate of fading channels, the maximum Doppler frequency shift f_D (or the static slots duration of α_n, i.e., L) will affect the sensing performance of the designed algorithm. In order to simulate time-varying fading channels, in the experiment the partitioned number is $K=5$ and the distribution variance is $\sigma^2=0.1$. By providing a random initial state, a realization of TVFF channel may be then generated from a specific TPM which is calculated from eqs. (10)–(13). The samples size M is set 10, the transitional rates (λ,μ) are configured to $((1/10T_F),(1/5T_F))$.

For realistic slow-varying channels, f_D may be assumed to smaller than 100 Hz. Thus, three typical configurations of L are considered in the experiments, i.e., $L=10$, 20, and 50. It is seen that the proposed algorithm, relying on joint estimations of time-varying fading gain and PUs state, can dramatically improve the sensing performance when operating in realistic TVFF channels. It is observed from Fig. 6 that a smaller L, corresponding to a relatively faster change rate of fading channel, may obtain less gain compared with ED. Taking $L=10$ for example, the achieved gain with regard to ED is about 6 dB when the probability of detections P_D surpasses 0.95. In comparison, the SNR benefit of the proposed method may even increase to 10 dB when L is increased to 20. Meanwhile, it is noted that, since the threshold configuration of ED can hardly exploit the underlying memory information of time-varying fading channels, L seems to have little impacts on its sensing performance.

This result is mainly contributed by the designed estimation reinforcement procedure of fading gains. To be specific, the updating of fading gain is essentially based on an initial PU state and subsequent Bayesian estimations by using accumulated observations. If the channel changes too fast, due to the shortened static length L, further refinements on the estimation of fading gain via the L-segment observations may become weakened. Accordingly, the errors in the initial estimation of PU state will become predominant. As a consequence, the estimation accuracy of the fading gain in the presence of a small L may be degraded, accompanying the achieved sensing gain.

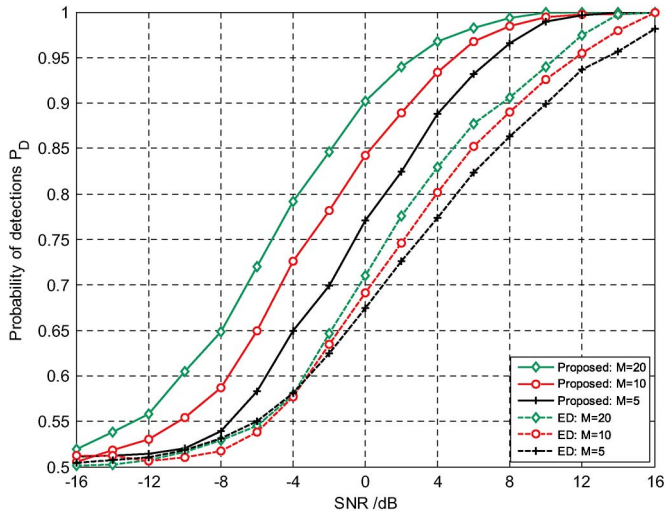

Fig. 7. Sensing performance of the presented joint estimation algorithm under different M. Notice that, $K=5$, $L=20$, and $(\lambda,\mu)=((1/10T_F),(1/5T_F))$.

E. Sampling Size M

As the adopted sensing strategy is based on a periodic-sensing framework, i.e., the sensing slot is followed by a transmission stage, the samples size M should be properly configured, in order to obtain a competitive sensing performance while maintaining the transmission efficiency of SUs. In this simulation, we configure the steady slots duration L to 20, the transitional rates (λ,μ) to $((1/10T_F),(1/5T_F))$ and the partitioning size K to 5.

Firstly, it is observed from Fig. 7 that the sensing performance of the joint estimation-based new algorithm is noticeably superior to ED in the presence of time-varying fading effects.

The detection gains of the new scheme may even approach 6 dB in the high SNRs region with a high detections probability P_D (i.e., $P_D = 0.98$). Besides, it is seen that increasing the samples size M is an effective way to enhance detection performances of both two methods. With a larger samples size M, more sufficient information of received signals can be utilized and, therefore, more accurate estimations may be derived. For example, if M is increased from 10 to 20, a detection gain of 2.5 dB will be achieved by the new algorithm in high SNRs region (i.e., $P_D > 0.99$), and this sensing gain may be further enlarged to 3.5 dB in the moderate SNRs region (i.e., $P_D > 0.9$). Nevertheless, it should be noteworthy that the increasing of samples size implies the decrease of transmission efficiency, as the sensing-transmission period (i.e., T_F) is fixed. In practice, the sensing time will also be prolonged with a large M. Therefore, this parameter configuration should be compromised in accordance with specific scenarios.

F. Comparative Analysis

In this experiment, the covariance-based sensing scheme is investigated for the purpose of comparative analysis, which is proven to be relatively robust to slow-varying fading effects [16]. In the CAV method, the smoothing factor is chosen to 12, and the threshold is calculated by maximizing the total probability of detections, like in eq. (17). For the DSS based new scheme, the static length is $L = 20$.

In typical scenarios, the received signal is considered to be correlated. Note that, in practice, either a narrow-band PU signal (e.g., generated by over-sampling techniques) or the correlated noise (e.g., produced from band-pass filtering) may arouse the temporal correlations. In the simulation, the BPSK scheme is adopted with each symbol modulated by a Gaussian shaper $p(m)$ of N_s samples. It is seen from experimental simulations that, with realistic TVFF gains, the proposed method is superior to the CAV method. When the sampling size M is 300 and $N_s = 11$, a detection gain of 2 dB can be achieved by the new scheme, as shown by Fig. 8. The main reason of this advantage is that, although the two methods are all premised on the statistical analysis, the CAV method may unfortunately fail to make the best of the time-varying property, accompanying the underlying *memory* of fading channels which may be further exploited to enhance the detection performance.

In some other specific applications, unfortunately, the correlations of PU signals may become insignificant. In such situations, the CAV method, which essentially utilizes the statistical correlation of PU signals [5], [16], may fail to detect PU signals unfortunately. In comparison, from Fig. 8, the sensing performance of the DSS-based method will be basically unaffected. Therefore, the new method may relieve specific statistical assumptions on received signals and may hence have more widespread applications.

G. Practical Considerations

In the analysis, a total detection probability is adopted, i.e., $P(H_0)(1 - P_f) + P(H_1)P_d$. Notice that, the threshold-based techniques (e.g., ED), which are usually applied to another

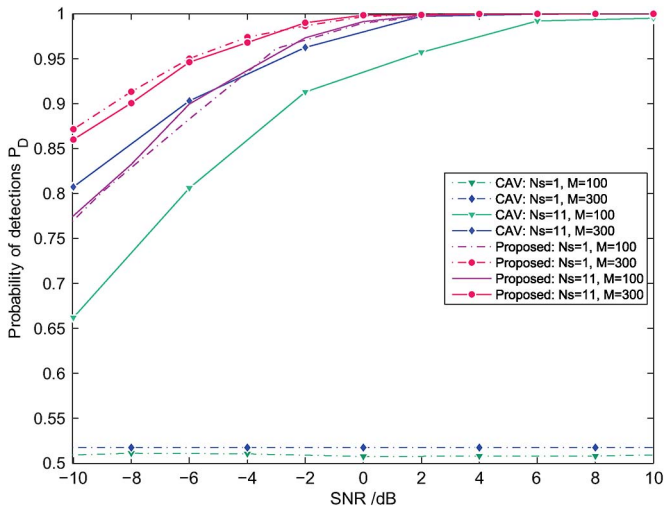

Fig. 8. Sensing performance of different methods in the presence of TVFF channels. Notice that, $K = 5$, $L = 20$, and $(\lambda, \mu) = ((1/10T_F), (1/5T_F))$. For CAV method, the averaging length is set to 12.

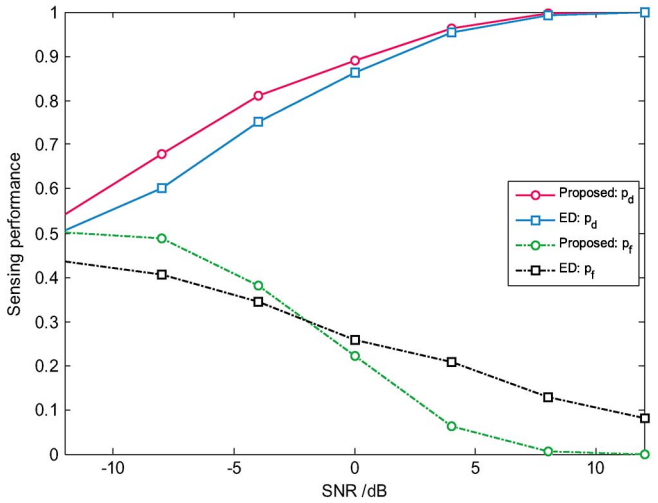

Fig. 9. The detection probability and the false-alarm probability of two summed-energy based sensing schemes. Notice that, $K = 5$, $M = 10$, $L = 20$, and $(\lambda, \mu) = ((1/10T_F), (1/5T_F))$.

different criterion, i.e., the Neyman–Pearson criterion, seems to be no longer suitable to the proposed joint estimation-based sensing scheme. With a new Bayesian MAP approach and the objective of maximizing the compound probability P_D, the false-alarm probability would also become not fixed.

Taking SNR $= 8$ dB for example, it may be concluded from Fig. 7 that the false alarm probability P_f of the proposed scheme is smaller than $(1 - 0.99)/P(H_0) = 0.02$, and smaller than $(1 - 0.906)/P(H_0) = 0.19$ for ED. Furthermore, we may investigate P_d and P_f separately under the same configuration. From the numerically derived results in Fig. 9, when SNR is set to 4 dB, the detection probability of the new method is $P_d = 0.962$ and the false alarm probability is $P_f = 0.052$. In comparison, the detection probability of ED is $P_d = 0.953$ and the false alarm probability is only $P_f = 0.218$. When SNR $=$ 8 dB, $P_d = 0.997$, and $P_f = 0.004$ for the new scheme, while $P_d = 0.993$ and $P_f = 0.132$ for ED. By dramatically reducing

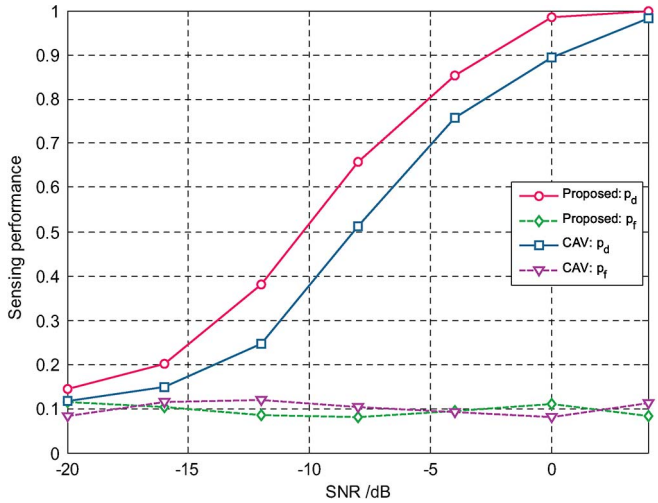

Fig. 10. The detection probability for a target $P_f = 0.1$. Here, $M = 100$, $K = 5$, $L = 20$, and $(\lambda, \mu) = ((1/10T_F), (1/5T_F))$. For CAV method, the averaging length is set to 11.

false-alarms, the proposed scheme may promote the spectrum utilization of unused primary bands significantly. Therefore, the SU' throughput of the new method is superior to ED. Note that, however in low-SNR regions (e.g., SNR ≤ 0 dB), the advantage of the new method seems to be insignificant.

Although the new scheme is premised essentially on a Bayesian MAP criterion, its performance could also be evaluated under another criterion (i.e., the Neyman–Pearson criterion) like some classical algorithms. Since the estimated fading channel cannot be fully exploited by setting a simple threshold according to a predefined P_f, the detection probability P_d of our new method will become comparable to ED in such a case. This is easy to understand, as the observation in our new DSM is actually the summed-energy as in eq. (14). Even so, as another extra gift of sensing process, it should be noted that the recovered fading channel (e.g., with the estimation MSE $=$ 0.008 when SNR $= 10$ dB and $M = 100$) may be of great significance to subsequent optimizations or strategy selections. Based on numerical experiments, we may also consider the CAV method for comparisons, where a predefined P_f is set to 0.1 and the over-sampling factor is $N_s = 10$. It is seen from simulation results in Fig. 10 that, given a comparable P_f, the proposed scheme may surpass the CAV method as far as the single P_d is considered. To be specific, a detection gain of larger than 2 dB could be acquired by the new method when $P_d > 0.9$.

V. Conclusion

In this paper, we developed a new spectrum sensing algorithm for realistic TVFF channels within the framework of Bayesian statistical inference. By fully utilizing the dynamic behaviors of both PU state and the time-variant fading gains, a novel DSM is formulated to thoroughly characterize the sensing problem. On this basis, an iteratively implemented scheme is designed and the spectrum sensing is efficiently realized by estimating the time-varying fading gain and unknown PU state jointly. The sensing performances of this design scheme, with various different parameter configurations, are thoroughly investigated. Experimental simulations have validated the new algorithm. The proposed DSM and joint estimation algorithm may provide a promising solution for spectrum sensing in more realistic TVFF channels, which can significantly enhance the sensing performance even in distributed CR networks where the cooperative sensing may become infeasible.

Appendix
Extension to Complex Signals

(1) We firstly consider the case of H_1. For clarity, the mth complex signal in the nth slot is denoted by $u(n,m) = u_c(n,m) + ju_s(n,m)$ and the complex fading gain is $\alpha(n) = \alpha_c(n) + j\alpha_s(n)$, the received signal may be written to:

$$\begin{aligned} y(n) &= \sum_{m=0}^{M-1} |[\alpha_c(n) + j\alpha_s(n)] \times [u_c(n,m) + ju_s(n,m)] \\ &\qquad + [z_c(n,m) + jz_s(n,m)]|^2 \\ &= \sum_{m=0}^{M-1} [\alpha_c(n)u_c(n,m) - \alpha_s(n)u_s(n,m) + z_c(n,m)]^2 \\ &\quad + \sum_{m=0}^{M-1} [\alpha_c(n)u_s(n,m) + \alpha_s(n)u_c(n,m) + z_s(n,m)]^2 \\ &= y_s(n) + y_c(n), \end{aligned} \tag{44}$$

where $j = \sqrt{-1}$ is the imaginary number. The component $y_s(n)$ may be further reformatted as eq. (45), shown at the bottom of the page.

When the sample size M is large (e.g., $M > 100$), it suffices to prove that the first term $y_{s,1}(n)$ may tend to be a constant (if the complex signals of constant modulus are considered, e.g., QPSK), which is basically independent of different time

$$\begin{aligned} y_s(n) = &\underbrace{\sum_{m=0}^{M-1} [\alpha_c^2(n)u_c^2(n,m) + \alpha_s^2(n)u_s^2(n,m) - 2\alpha_c(n)u_c(n,m)\alpha_s(n)u_s(n,m)]}_{y_{s,1}(n)} + \underbrace{\sum_{m=0}^{M-1} z_s^2(n,m)}_{y_{s,2}(n)} \\ &\underbrace{+ 2 \times \sum_{m=0}^{M-1} [\alpha_c(n)u_c(n,m) - \alpha_s(n)u_s(n,m)] \times z_c(n,m)}_{y_{s,3}(n)} \end{aligned} \tag{45}$$

indexes n. The second term, according to the central limit theorem (CLT), will become a Gaussian random variable, with the mean and variance specified by $\mathbb{E}\{y_{s,2}(n)\}$ and $\mathbb{V}\{y_{s,2}(n)|\alpha_c(n),\alpha_s(n)\}$, respectively. The third term $y_{s,3}(n)$, as the summation of M independent random variables, is also a Gaussian variable, whose mean and variance are denoted by $\mathbb{E}\{y_{s,3}(n)|\alpha_c(n),\alpha_s(n)\}$ and $\mathbb{V}\{y_{s,3}(n)|\alpha_c(n),\alpha_s(n)\}$, repetitively.

In practice, we may easily note the cross-correlation function between $y_{s,2}(n)$ and $y_{s,3}(n)$ equals approximately to zero, i.e., $\mathcal{R}_{y_{s,3},y_{s,3}}(n') \triangleq \mathbb{E}\{y_{s,2}(n)y_{s,3}(n-n')\} \to 0$ (for $n' \geq 0$). It is therefore considered that the second term and the third term remain also independent of each other. Thus, $y_s(n)$ is also a Gaussian variable, i.e.,

$$p\left(y_s(n)|\alpha_c(n),\alpha_s(n),H_1\right) \sim \mathcal{N}\{\mathbb{E}\{y_s(n)|\alpha_c(n),\alpha_s(n),H_1\},\mathbb{V}\{y_s(n)|\alpha_c(n),\alpha_s(n),H_1\}\}, \tag{46}$$

with its mean and variance determined by

$$\begin{aligned}
&\mathbb{E}\left\{y_s(n)|\alpha_c(n),\alpha_s(n),H_1\right\} \\
&\quad = \mathbb{E}\left\{y_{s,1}(n)|\alpha_c(n),\alpha_s(n),H_1\right\} + \mathbb{E}\left\{y_{s,2}(n)\right\} \\
&\quad = \sum_{m=0}^{M-1}\left\{\alpha_c^2(n)\mathbb{E}\{u_c^2(n,m) + \alpha_s^2(n)\mathbb{E}\left\{u_s^2(n,m)\right\}\right. \\
&\qquad\qquad \left. - 2\alpha_c(n)\alpha_s(n)\mathbb{E}\left[u_c(n,m)u_s(n,m)\right]\right\} + M\sigma_z^2 \\
&\quad \overset{(a)}{=} ME_s\left[\alpha_c^2(n) + \alpha_s^2(n)\right] + M\sigma_z^2,
\end{aligned} \tag{47}$$

and

$$\begin{aligned}
&\mathbb{V}\left\{y_s(n)|\alpha_c(n),\alpha_s(n),H_1\right\} \\
&\quad = \mathbb{V}\left\{y_{s,2}(n)\right\} + \mathbb{V}\left\{y_{s,3}(n)|\alpha_c(n),\alpha_s(n),H_1\right\} \\
&\quad = \mathbb{E}\left\{\left[\sum_{m=0}^{M-1} z_s^2(n,m) - \sigma_z^2\right]^2\right\} \\
&\qquad + 4\mathbb{E}\left\{\left\{\sum_{m=0}^{M-1}\left[\alpha_c(n)u_c(n,m) - \alpha_s(n)u_s(n,m)\right]\right.\right. \\
&\qquad\qquad \left.\left. \times z_c(n,m)\right\}^2\right\} \\
&\quad = 4M\sigma_z^4 + 4M\sigma_z^2E_s^2 \times \left[\alpha_c^2(n) + \alpha_s^2(n)\right],
\end{aligned} \tag{48}$$

respectively, where E_s denotes the average power of in-phase components, i.e.,

$$E_s \triangleq \mathbb{E}\left\{u_c^2(n,m)\right\} = \mathbb{E}\left\{u_s^2(n,m)\right\}. \tag{49}$$

In eq. (47), (a) holds for the two independent components, i.e., $\mathbb{E}\{u_c(n,m)u_s(n,m)\} = 0$. Note that, for other signals of non-constant modulus (e.g., M-QAM), the first term $y_{s,1}(n)$ may also become a Gaussian variable when M is large, however the above analysis may be carried out in a similar manner.

Similarly, the term $y_c(n)$ is also a Gaussian variable, whose mean and variance is equivalent to that of $y_s(n)$. Given y_c and $y_s(n)$ involve a group of same noise variables, then the likelihood distribution of observation $y(n)$ is also a Gaussian variable, i.e.,

$$p\left(y(n)|\alpha_c(n),\alpha_s(n),H_1\right) \sim \mathcal{N}\{\mathbb{E}\left\{y(n)|\alpha_c(n),\alpha_s(n),H_1\right\},\mathbb{V}\left\{y(n)|\alpha_c(n),\alpha_s(n),H_1\right\}\}, \tag{50}$$

where the mean and variance are specified by eqs. (51) and (52), respectively.

$$\mathbb{E}\{y(n)|\alpha_c(n),\alpha_s(n),H_1\} = 2\times\mathbb{E}\{y_s(n)|\alpha_c(n),\alpha_s(n),H_1\}, \tag{51}$$

$$\mathbb{V}\{y(n)|\alpha_c(n),\alpha_s(n),H_1\} = 2\times\mathbb{V}\{y_s(n)|\alpha_c(n),\alpha_s(n),H_1\}. \tag{52}$$

(2) When the PU signal is absent (i.e., H_0), then the likelihood function $p(y(n)|H_0)$ will also follow a central chi-square distribution. Note that, with the complex signal, however the DoF of relative distributions will become $2M$ accordingly.

Thus, the likelihood densities involved in eqs. (33) and (37)–(40) may be easily obtained and, from the algorithm elaborations, the proposed algorithm can be extended to complex signals. Meanwhile, it is noted that the complexity may be slightly increased due to additional computations of eqs. (47) and (48).

ACKNOWLEDGMENT

We greatly thank anonymous reviewers for their constructive comments and helpful feedback that allowed us to improve the paper significantly.

REFERENCES

[1] J. Mitola and G. Q. Maguire, "Cognitive radio: Making software radios more personal," *IEEE Pers. Commun.*, vol. 6, no. 4, pp. 13–18, Aug. 1999.
[2] S. Haykin, "Cognitive radio: Brain-empowered wireless communications," *IEEE J. Sel. Areas Commun.*, vol. 23, no. 2, pp. 201–220, Feb. 2005.
[3] Y. C. Liang, K. C. Chen, G. Y. Li, and P. Mahonen, "Cognitive radio networking and communications: An overview," *IEEE Trans. Veh. Technol.*, vol. 60, no. 7, pp. 3386–3407, Sep. 2011.
[4] L. Lu, X. W. Zhou, U. Onunkwo, and G. Y. Li, "Ten years of cognitive radio technology," *EURASIP J. Wireless Commun. Netw.*, vol. 28, pp. 1–16, 2012.
[5] J. Ma, G. Y. Li, and B. H. Juang, "Signal processing in cognitive radio," *Proc. IEEE*, vol. 97, no. 5, pp. 805–823, May 2009.
[6] E. Axell, G. Leus, E. G. Larsson, and H. V. Poor, "Spectrum sensing for cognitive radio: State-of-the-art and recent advances," *IEEE Signal Process. Mag.*, vol. 29, no. 3, pp. 101–116, May 2012.
[7] F. F. Digham, M. S. Alouini, and M. K. Simon, "On the energy detection of unknown signals over fading channels," in *Proc. IEEE ICC*, Anchorage, AK, USA, May 2003, vol. 5, pp. 3575–3579.
[8] H. S. Chen, W. Gao, and D. G. Daut, "Signature based spectrum sensing algorithms for IEEE 802.22 WRAN," in *Proc. IEEE ICC*, Glasgow, U.K., Jun. 2007, pp. 6487–6492.
[9] R. Tandra and A. Sahai, "Fundamental limits on detection in low SNR under noise uncertainty," in *Proc. WCSSP*, Jun. 2005, pp. 464–469.
[10] S. Haykin, D. J. Thomson, and J. H. Reed, "Spectrum sensing for cognitive radio," *Proc. IEEE*, vol. 97, no. 5, pp. 849–877, May 2009.

[11] P. D. Sutton, K. E. Nolan, and L. E. Doyle, "Cyclostationary signature in practical cognitive radio applications," *IEEE J. Sel. Areas Commun.*, vol. 26, no. 1, pp. 13–24, Jan. 2008.
[12] A. Sahai, N. Hoven, and R. Tandra, "Some fundamental limits on cognitive radio," in *Proc. 42nd Allerton Conf. Commun. Control Comput.*, Monticello, IL, USA, Oct. 2004.
[13] Z. Tian and G. B. Giannakis, "A wavelet approach to wideband spectrum sensing for cognitive radios," in *Proc. IEEE Conf. CROWNCOM*, Mykonos Island, Greece, Jun. 2006, pp. 1–5.
[14] Z. Tian and G. B. Giannakis, "Compressed sensing for wideband cognitive radios," in *Proc. IEEE ICASSP*, Honolulu, HI, USA, Apr. 2007, pp. 1357–1360.
[15] Y. H. Zeng and Y. C. Liang, "Eigenvalue-based spectrum sensing algorithms for cognitive radio," *IEEE Trans. Commun.*, vol. 57, no. 6, pp. 1784–1793, Jun. 2009.
[16] Y. H. Zeng and Y. C. Liang, "Spectrum-sensing algorithms for cognitive radio based on statistical covariances," *IEEE Trans. Veh. Technol.*, vol. 58, no. 4, pp. 1804–1815, May 2009.
[17] X. W. Zhou, Y. Li, Y. H. Kwon, and A. C. K. Soong, "Detection timing and channel selection for periodic spectrum sensing in cognitive radio," in *Proc. IEEE GLOBECOM*, New Orleans, LA, USA, Nov. 30–Dec. 4, 2008, pp. 1–5.
[18] J. Ma and Y. Li, "A probability-based spectrum sensing scheme for cognitive radio," in *Proc. IEEE ICC*, Beijing, China, May 2008, pp. 3416–3420.
[19] V. Lenders, S. Heimlicher, M. May, and B. Plattner, "An empirical study of the impact of mobility on link failures in an 802.11 *ad hoc* network," *IEEE Wireless Commun.*, vol. 15, no. 6, pp. 16–21, Dec. 2008.
[20] W. Haselmayr, D. Schellander, and A. Springer, "Iterative channel estimation and turbo equalization for time-varying channels in a coded OFDM-LTE system for 16-QAM and 64-QAM," in *Proc. IEEE 21st Int. Symp. PIMRC*, Istanbul, Turkey, Sep. 2010, pp. 614–618.
[21] E. G. Larsson and G. Regnoli, "Primary system detection for cognitive radio: Does small-scale fading help?" *IEEE Commun. Lett.*, vol. 11, no. 10, pp. 799–801, Oct. 2007.
[22] A. Ghasemi and E. S. Sousa, "Collaborative spectrum sensing for opportunistic access in fading environments," in *Proc. IEEE Symp. New Frontiers DySPAN*, Baltimore, MD, USA, Nov. 2005, pp. 131–136.
[23] W. Zhang, R. K. Mallik, and K. B. Letaief, "Cooperative spectrum sensing optimization in cognitive radio networks," in *Proc. IEEE ICC*, Beijing, China, May 2008, pp. 3411–3415.
[24] K. B. Letaief and W. Zhang, "Cooperative communications for cognitive radio networks," *Proc. IEEE*, vol. 97, no. 5, pp. 878–893, May 2009.
[25] F. F. Digham, M. S. Alouini, and M. K. Simon, "On the energy detection of unknown signals over fading channels," *IEEE Trans. Commun.*, vol. 55, no. 1, pp. 21–24, Jan. 2007.
[26] B. Sklar, "Rayleigh fading channels in mobile digital communication systems Part I: Characterization," *IEEE Commun. Mag.*, vol. 35, no. 7, pp. 90–100, Jul. 1997.
[27] J. G. Proakis, *Digital Communications,* 3rd ed. New York, NY, USA: McGraw-Hill, 1995.
[28] H. S. Wang and N. Moayeri, "Finite-state Markov channel: A useful model for radio communication channels," *IEEE Trans. Veh. Technol.*, vol. 44, no. 1, pp. 163–171, Feb. 1995.
[29] P. M. Djuric *et al.*, "Particle filtering," *IEEE Signal Process. Mag.*, vol. 20, no. 5, pp. 19–38, Sep. 2003.
[30] Z. G. Yang and X. D. Wang, "A sequential Monte Carlo blind receiver for OFDM systems in frequency-selective fading channels," *IEEE Trans. Signal Process.*, vol. 50, no. 2, pp. 271–280, Feb. 2002.
[31] B. Vujitic, N. Cackov, and S. Vujitic, "Modeling and characterization of traffic in public safety wireless network," in *Proc. Int. Symp. Perform. Eval. Comput. Telecommun. Syst.*, Edinburgh, U.K., Jul. 2005, pp. 213–223.
[32] B. Li, Z. Zhou, and W. X. Zou, "Interference mitigation between ultra-wideband sensor network and other legal systems," *EURASIP J. Wireless Commun. Netw.*, Jan. 2010, Article number: 290306.
[33] P. Sadeghi, R. Kennedy, P. Rapajic, and R. Shams, "Finite-state Markov modeling of fading channels: A survey of principles and applications," *IEEE Signal Process. Mag.*, vol. 25, no. 5, pp. 57–80, Sep. 2008.
[34] K. E. Baddour and N. C. Beaulieu, "Autoregressive modeling for fading channel simulation," *IEEE Trans. Wireless Commun.*, vol. 4, no. 4, pp. 1650–1662, Jul. 2005.
[35] R. H. Clarke, "A statistical theory of mobile-radio reception," *Bell Syst. Tech. J.*, vol. 47, no. 6, pp. 957–1000, Jul./Aug. 1968.
[36] H. S. Wang and P. Chang, "On verifying the first order Markovian assumption for a Rayleigh fading channel model," *IEEE Trans. Veh. Tech.*, vol. 45, no. 2, pp. 353–357, May 1996.
[37] F. Babich and G. Lombardi, "A Markov model for the mobile propagation channel," *IEEE Trans. Veh. Technol.*, vol. 49, no. 1, pp. 63–73, Jan. 2000.
[38] W. Turin and R. van Nobelen, "Hidden Markov modeling of flat fading channels," *IEEE J. Select. Areas Commun.*, vol. 16, no. 9, pp. 1809–1817, Dec. 1998.
[39] W. B. Davenport, Jr. and W. L. Root, *An Introduction to the Theory of Random Signals and Noise*. New York, NY, USA: IEEE Press, 1958.
[40] C. Tellambura and A. D. S. Jayalath, "Generation of bivariate Rayleigh and Nakagami-m fading envelopes," *IEEE Commun. Lett.*, vol. 4, no. 5, pp. 170–172, Dec. 2000.
[41] X. F. Dong and N. C. Beaulieu, "Average level crossing rate and average fade duration of selection diversity," *IEEE Commun. Lett.*, vol. 5, no. 10, pp. 396–398, Oct. 2010.
[42] C. T. Christopher and N. C. Beaulieu, "On first-order Markov modeling for the Rayleigh fading channel," *IEEE Trans. Commun.*, vol. 48, no. 12, pp. 2032–2040, Dec. 2000.
[43] B. Li, Z. Zhou, and A. Nallanathan, "Joint estimation based spectrum sensing for cognitive radios in time variant flat fading channel," in *Proc. IEEE Globecom*, Atlanta, GA, USA, Dec. 2013, pp. 1–6.
[44] A. Doucet, "On sequential simulation-based methods for Bayesian filtering," *Statist. Comput.*, vol. 10, no. 3, pp. 197–208, Jul. 2000.
[45] Y. C. Liang, Y. H. Zeng, E. C. Y. Peh, and T. H. Anh, "Sensing–throughput tradeoff for cognitive radio networks," *IEEE Trans. Wireless Commun.*, vol. 7, no. 4, pp. 1326–1337, Apr. 2008.
[46] B. Haible and T. Papanikolaou, "Fast multiple-precision evaluation of series of rational numbers," in *Proc. 3rd Int. ANTS*, Portland, OR, USA, Jun. 21th–25th, 1998, pp. 338–350.

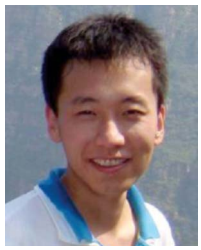

Bin Li received the bachelor's degree in electrical information engineering from Beijing University of Chemical Technology, Beijing, China, in 2007 and the master's degree in communication and information engineering from Beijing University of Posts and Telecommunications (BUPT), Beijing, in 2009. He is currently working toward the Ph.D. degree in communication and information systems with BUPT. He has published more than 40 journal and conference papers. His current research interests are focused on statistical signal processing algorithms for ultra-wideband, wireless sensor networks, millimeter-wave communications, and cognitive radios and channel modeling. Dr. Li served as a regular reviewer for the IEEE SIGNAL PROCESSING LETTERS, IEEE TRANSACTIONS ON COMMUNICATIONS, IEEE TRANSACTIONS ON SIGNAL PROCESSING, and IEEE TRANSACTIONS ON SYSTEMS, MAN, AND CYBERNETICS. He was a recipient of the 2011 ChinaCom Best Paper Award and the 2010 and 2011 BUPT Excellent Ph.D. Student Award Foundation.

Chenglin Zhao received the bachelor's degree in radio-technology from Tianjin University, Tianjin, China, in 1986 and the master's degree in circuits and systems and the Ph.D. degree in communication and information system from Beijing University of Posts and Telecommunications (BUPT), Beijing, China, in 1993 and 1997, respectively. He currently serves as a Professor at BUPT. His research is focused on emerging technologies of short-range wireless communication, cognitive radios, and 60 GHz millimeter-wave communications.

Mengwei Sun received the bachelor's degree in communication engineering from Civil Aviation University of China, Tianjin, China, in 2011. She is currently working toward the Ph.D. degree with the School of Information and Communication Engineering, Beijing University of Posts and Telecommunications, Beijing, China. Her current research interests focus on signal processing for cognitive radios and 60-GHz millimeter-wave communications.

Zheng Zhou (M'05) received the bachelor's degree in electrical engineering from the Harbin Institute of Military Engineering, Harbin, China, in 1967 and the master's and Ph.D. degrees in electrical engineering from Beijing University of Posts and Telecommunications (BUPT), Beijing, China, in 1982 and 1988, respectively.

He is currently a Professor at BUPT. Supported by the Hong Kong Telecom International Postdoctoral Fellowship, he was a Visiting Research Fellow at the Information Engineering Department, Chinese University of Hong Kong, Hong Kong, from 1993 to 1995. He was also the Vice-Dean at the School of Telecommunication Engineering, BUPT, from 1998 to 2003 and was the Invited Overseas Researcher in Japan Kyocera DDI Future Communication Research Institute (supported by the Japan Key Technology Center) in 2000.

Prof. Zhou served as a member of the Technical Subcommittee on Cognitive Networks (TCCN), IEEE Communications Society, the International Steering Committee Member for the IEEE ISCIT during 2003–2010 (International Symposium on Communications and Information Technologies), and the TPC Co-Chair for the IEEE ISCIT 2005. He was also the General Vice Chair for the IEEE ChinaCom 2006 (the first international conference on communications and networking in China) and the Steering Committee Member for the IEEE ChinaCom 2007. He is the voting member and contributor of the IEEE 802.15 Task Group (TG3a and TG4a), Senior Member of China Institution of Communications (CIC), Radio Application and Management Technical Committee Member of CIC, Senior Member of China Computer Federation (CCF), Sensor Network Technical Committee Member of CCF, *H*-Subcommittee Member of China Radio Interference Standard Technology Committee, the General Secretary of China UWB Forum, and the General Secretary of China Bluetooth Forum.

Arumugam Nallanathan (S'97–M'00–SM'05) is a Professor of wireless communications at the Department of Informatics, King's College in London (University of London), London, U.K. He served as the Head of Graduate Studies, School of Natural and Mathematical Sciences, King's College London, in December 2011. He was an Assistant Professor at the Department of Electrical and Computer Engineering, National University of Singapore, from August 2000 to December 2007. His research interests include 5G technologies, millimeter wave communications, cognitive radio, and relay networks. In these areas, he co-authored more than 200 papers.

Dr. Nallanathan is a Distinguished Lecturer of the IEEE Vehicular Technology Society. He is an Editor of the IEEE TRANSACTIONS ON COMMUNICATIONS and IEEE TRANSACTIONS ON VEHICULAR TECHNOLOGY. He was an Editor of the IEEE TRANSACTIONS ON WIRELESS COMMUNICATIONS (2006–2011), IEEE WIRELESS COMMUNICATIONS LETTERS, and IEEE SIGNAL PROCESSING LETTERS and a Guest Editor of *EURASIP Journal on Wireless Communications and Networks*: Special issue on UWB Communication Systems-Technology and Applications (2006). He currently serves as the Chair for the Signal Processing and Communication Electronics Technical Committee of the IEEE Communications Society. He served as the Technical Program Co-Chair (MAC track) for the IEEE WCNC 2014, Co-Chair for the IEEE GLOBECOM 2013 (Communications Theory Symposium), Co-Chair for the IEEE ICC 2012 (Signal Processing for Communications Symposium), Co-Chair for the IEEE GLOBECOM 2011 (Signal Processing for Communications Symposium), Technical Program Co-Chair for the IEEE International Conference on UWB 2011 (IEEE ICUWB 2011), Co-Chair for the IEEE ICC 2009 (Wireless Communications Symposium), Co-Chair for the IEEE GLOBECOM 2008 (Signal Processing for Communications Symposium), and General Track Chair for the IEEE VTC 2008. He was a co-recipient of the Best Paper Award presented at the 2007 IEEE International Conference on Ultra-Wideband (ICUWB2007). He was also a recipient of the IEEE Communications Society Signal Processing and Communications Electronics (SPCE) Outstanding Service Award in 2012 and Radio Communications Committee (RCC) Outstanding Service Award in 2014.